MATHEMATICAL MODELING OF A DIRECT ETHANOL FUEL CELL (DEFC)

R.S. Gomes, ranon.souza@ufrgs.br[1]
A.L. De Bortoli, dbortoli@mat.ufrgs.br[1]

[1]Universidade Federal do Rio Grande do Sul, Av. Bento Gonçalves 9500, Porto Alegre - RS, 91509-900, Brazil

Abstract: *This work develops a three-dimensional mathematical model able to predict the flow in all layers of the DEFC. In addition, the model estimates the operating voltage of the cell considering all losses overpotentials, which are obtained from the parameters of the cell and of the flow in the channel, in the diffusion layer and in the surface of the electrocatalyst. A code in Fortran90 was developed for the solution of the three-dimensional mathematical model. The finite difference method was used for the discretization, and the numerical simulations were realized using the simplified three-stage Runge-Kutta method. Obtained results are in agreement with experimental data found in the literature for various cell operation temperatures. In this way, this work contributes with the development of a model for DEFCs taking into account all losses overpotentials, providing a better understanding of the physical and chemical behavior within the cell.*
Keywords: *Fuel Cell, Ethanol, Mathematical modeling, Numerical simulation*

1. INTRODUCTION

There is growing interest in renewable energy sources worldwide. Concerns about global warming and energy generation that is not fully dependent on petroleum has taken attention of researchers. Many of these sources can be continuously produced, such the biofuels. Alternative sources such as the hydric, solar and eolian have been used for energy production; however, these sources do not have complete confidence and in some cases have high cost of implementation. In the case of biofuels, great expectations exist about its use as alternative fuels. A device able to utilize more efficiently the energy of biofuels is the fuel cell. The fuel cell is an electrochemical device capable of converting chemical energy of fuel directly into electrical energy. Ethanol is an attractive fuel for use in fuel cells for automotive and electronic applications. Much of the work performed have focused on the use of hydrogen and methanol in fuel cells. One of the main advantages of the ethanol in relation to methanol and hydrogen, is the pre-established infrastructure compared to hydrogen and the low toxicity as compared to methanol.

Mathematical models are needed to optimize the design of fuel cells for development of power systems. To understand and improve the performance of DEFC systems, several mathematical models have been proposed to estimate the relation between voltage and current density (Le *et al.*, 2010). However, most of the work reported in the literature employ one-dimensional models to estimate the flow in the different layers of DEFC (Abdullah *et al.*, 2014). In a recent paper, Abdullah *et al.* (2014) made a review of direct ethanol fuel cell and reported that they found just one work (Sarris *et al.*, 2006) focused on three-dimensional models. Therefore, among the major advances in the development and improvement of DEFC cited by Abdullah *et al.* (2014), there is the urgent need to develop a multi-phase and a multi-dimensional mathematical model that can capture the complex physical and chemical behavior of real DEFC systems. Thus, this work proposes a three-dimensional model for calculating the flow in all layers of the DEFC.

2. ELECTROCHEMICAL REACTIONS INSIDE THE DEFC

A DEFC follows the most basic form of proton exchange membrane fuel cell (PEMFC), that is: at the anode a fuel is electrochemically oxidized and generates protons and electrons, while at the cathode oxygen is reduced (Lamy *et al.*, 2009). A catalyst $PtRu/C$ is used at the anode and Pt/C at the cathode (Pramanik and Basu, 2010). The most common membrane used is the NAFION, produced by Dupont. The electrochemical reactions that take place inside the cell are given by:

$$C_2H_5OH + 3H_2O_{(l)} \rightarrow 2CO_2 + 12H^+ + 12e^- \quad \text{at the anode,} \tag{1}$$

$$3O_2 + 12H^+ + 12e^- \rightarrow 6H_2O_{(g)} \quad \text{at the cathode,} \tag{2}$$

corresponding to the overall reaction

$$C_2H_5OH + 3O_2 \rightarrow 2CO_2 + 3H_2O. \tag{3}$$

The complete oxidation of ethanol in carbon dioxide is complicated by the difficulty in breaking C-C bonds, forming intermediates which are adsorbed on the catalyst surface. Goel and Basu (2015) proposed three elementary steps for the electro-oxidation of ethanol, as follow:

$$C_2H_5OH + Pt \rightarrow (C_2H_5OH)_{ad,Pt} \rightarrow (CH_3CHO)_{ad,Pt} + 2H^+ + 2e^- \tag{4}$$

$$3H_2O + 3Ru \leftrightarrow 3(OH)_{ad,Ru} + 3H^+ + 3e^- \tag{5}$$

$$(CH_3CHO)_{ad,Pt} + 3(OH)_{ad,Ru} \rightarrow 2CO_2 + 7H^+ + 7e^- + Pt + 3Ru. \tag{6}$$

In the Fig. 1 is shown the DEFC modeled in this work. The mixture of ethanol and water is inserted into the anode side, which reacts to form carbon dioxide, protons, and electrons. The protons pass preferably to the cathode through the membrane and the electrons through an external circuit, providing a difference of potential. On the cathode side, the air reacts with the protons and electrons formed at the anode to produce water vapor (Al-Baghdadi, 2005).

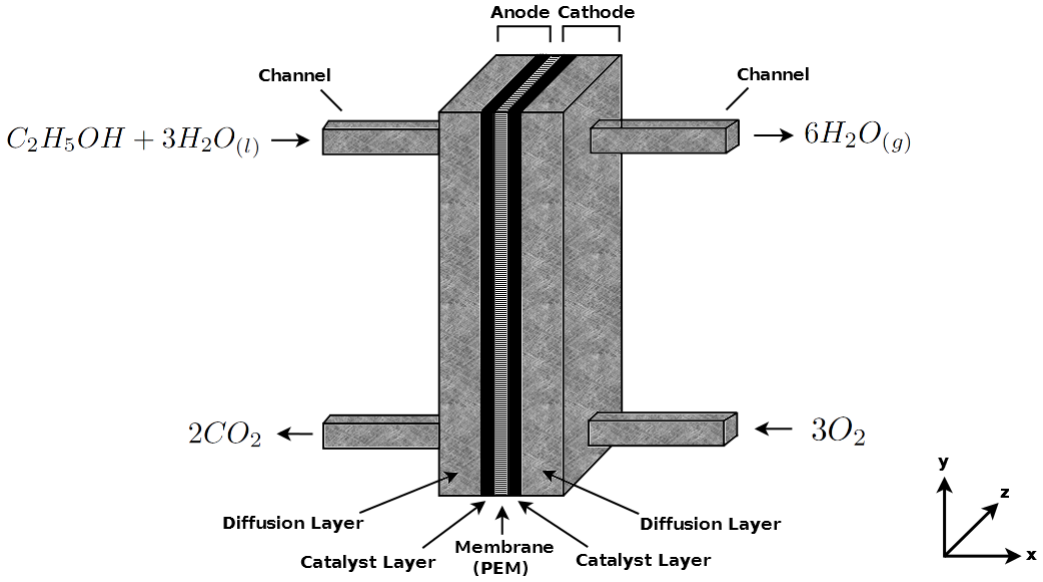

Fig. 1: Schematic diagram of three-dimensional DEFC

3. THREE-DIMENSIONAL MATHEMATICAL MODEL

For both anode and cathode, the equations have the same form. The fundamental equations are the continuity, momentum, and species conservation. These equations are written as:

3.1 Continuity equation:

$$\nabla \cdot u = 0. \tag{7}$$

3.2 Momentum equation:

$$\rho \frac{\partial u}{\partial t} + \rho u \cdot \nabla u = -\nabla p + \mu \nabla^2 u + \rho S_u, \tag{8}$$

where ρ is the density, u_i is the velocity in the direction i, with $i = 1, 2, 3$, μ is the viscosity and p is the pressure. Table 1 shows the source term S_u, where ε_d and ε_c are the porosities of the diffusion layer and of the catalyst layer, respectively, and k is the permeability. The fluid velocity in the diffusion and catalyst layers is described by Darcy's law (Liu and Wang, 2007).

Table 1: Source term S_u.

	flow channel	diffusion layer	catalyst layer
S_u	0	$-\varepsilon_d \frac{\mu}{k} u$	$-\varepsilon_c \frac{\mu}{k} u$

3.3 Species equations:

Each species k satisfies an equation of type

$$\rho \frac{\partial X_k}{\partial t} + \rho u \cdot \nabla X_k = \rho D_k^{\text{eff}} \nabla^2 X_k + S_k, \qquad \text{with} \quad \sum_k X_k = 1. \tag{9}$$

where X_k is the mole fraction of species k, D_k^{eff} is the effective diffusion coefficient and S_k is the sources term. The Table 2 and the Table 3 present the source term S_k, where j_a and j_c are the current density in the anode and cathode, M_{EtOH}, M_{H_2O}, M_{O_2} and M_{CO_2} are the molecular weights of ethanol, water, oxygen and carbon dioxide, respectively. The source term, S_k, is zero in the channels and in the diffusion layer.

Table 2: Source term S_k at the anode catalyst layer.

	ethanol	water	carbon dioxide
S_k	$-\frac{M_{EtOH}}{2F} j_a$	$-\frac{M_{H_2O}}{F} j_a$	$\frac{2M_{CO_2}}{7F} j_a$

Table 3: Source term S_k at the cathode catalyst layer.

	oxygen	water
S_k	$-\frac{M_{O_2}}{4F} j_c$	$\frac{M_{H_2O}}{2F} j_c$

The pressure comes from the Poisson's equation, which results from the derivative of the momentum equations in three dimensions. Similar results to pressure can be obtained from the equation

$$\frac{\partial p}{\partial t} + \rho c^2 \frac{\partial u}{\partial x} = 0, \tag{10}$$

where c is the speed of sound in the medium.

4. CELL VOLTAGE

One of the reasons of fuel cells modeling is to determine why the effective voltage differs from the thermodynamically predicted theoretical voltage. The overall cell voltage can be obtained using the following relationship:

$$V_{cell} = E^0_{cell} - (\eta_{act} + \eta_{ohm} + \eta_{con}), \tag{11}$$

where η_{act} are the losses due to activation, η_{ohm} are the losses due to ohmic resistance, η_{con} are the losses due to concentration, V_{cell} is the cell voltage, and E^0_{cell} is the reversible voltage of DEFC ($\sim$1.14 V).

The modified Butler-Volmer equation is used for determining the electrochemical reaction rate of electro-oxidation of ethanol in the anode catalyst and the reaction rate of oxygen reduction at the cathode catalyst (Pramanik and Basu, 2010; Andreadis *et al.*, 2006, 2008; Colmati *et al.*, 2006; Bard *et al.*, 2001; Heysiattalab and Shakeri, 2011):

$$j_a = j_0 \frac{X_{EtOH}}{X^{\text{ref}}_{EtOH}} \exp\left(\frac{\alpha_a n F}{RT} \eta_a\right), \tag{12}$$

$$j_c = j_0 \frac{X_{O_2}}{X^{\text{ref}}_{O_2}} \exp\left(\frac{\alpha_c n F}{RT} \eta_c\right), \tag{13}$$

where j_0 is the exchange current density (at the anode and cathode), X_{EtOH} is the ethanol mole fraction in the catalyst layer, X^{ref}_{EtOH} is the reference ethanol mole fraction, X_{O_2} is the mole fraction of oxygen in the catalyst layer, $X^{\text{ref}}_{O_2}$ is the reference oxygen mole fraction, α_a is the anode transfer coefficient, α_c is the cathode transfer coefficient, n is the number of electrons transferred, F is the Faraday constant, R is the universal gas constant, T is the temperature, η_a is the anode overpotential and η_c is the cathode overpotential.

4.1 Activation overpotential:

The relation between activation overpotential and current density at the anode is reported in the work of Pramanik and Basu (2010), and is given by:

$$\eta_{act,a} = \frac{RT}{\alpha_a n F} \ln[j_a (X_{EtOH} X_{H_2O})^{-0.25}], \tag{14}$$

where X_{H_2O} is the water mole fraction in the catalyst layer. The losses by activation at the cathode can be obtained from Tafel equation (Abdullah *et al.*, 2015; Yuan *et al.*, 2009; Farhat, 2004), resulting in:

$$\eta_{act,c} = \frac{RT}{\alpha_c n F} \ln\left(\frac{j_c}{j_0}\right). \tag{15}$$

4.2 Ohmic losses:

The ohmic loss is caused by the resistance to electron flow through the electrode, through the external circuit and due to the resistance to proton transport through the membrane. The ohmic losses can be written as

$$\eta_{ohm} = j_a \frac{t_m}{\sigma_m}, \tag{16}$$

where t_m is the thickness of membrane, and σ_m is the ionic conductivity for fully hydrated PEM, given by (Goel and Basu, 2015):

$$\sigma_m = 1268 \sigma^{\text{ref}}_m \left(\frac{1}{T_{\text{ref}}} - \frac{1}{T}\right). \tag{17}$$

4.3 Concentration overpotentials:

The model equation for concentration overpotential at the anode and cathode is given by, respectively (Pramanik and Basu, 2010; Abdullah *et al.*, 2015; Andreadis *et al.*, 2008):

$$\eta_{con,a} = \left(\frac{RT}{\alpha_a nF}\right) \ln\left(\frac{j_a}{j_0(1+j_a)}\right), \tag{18}$$

$$\eta_{con,c} = \left(\frac{RT}{\alpha_c nF}\right) \ln\left(\frac{j_c}{j_0(1-j_c N)}\right). \tag{19}$$

The parameters used for solving the model equations for DEFC are listed in the Table 4.

Table 4: Parameters used in the model of the DEFC at 315K.

Parameter	Unit	Present model	Reference
k_{O_2}	cm^2	1.76×10^{-7}	Ge and Liu (2006)
k_{H_2O}	cm^2	1.0×10^{-7}	Ge and Liu (2006)
μ_{O_2}	g $cm^{-1}s^{-1}$	2.05×10^{-5}	Ge and Liu (2006)
μ_{H_2O}	g $cm^{-1}s^{-1}$	4.061×10^{-9}	Suresh and Jayanti (2011)
R	J mol^{-1} K^{-1}	8.3144	Pramanik and Basu (2010)
F	Coulomb mol^{-1}	96,487	Pramanik and Basu (2010)
σ_m	S cm^{-1}	0.1416	Abdullah *et al.* (2015)
t_m	cm	0.00145	Pramanik and Basu (2010)
t_c	cm	0.001	Suresh and Jayanti (2011)
ε_d	dimensionless	0.65	Suresh and Jayanti (2011)
ε_c	dimensionless	0.4	Kareemulla and Jayanti (2009)
α_a	dimensionless	0.08	Suresh and Jayanti (2011)
α_c	dimensionless	0.1	Pramanik and Basu (2010)
j_0	mA cm^{-2}	0.03	Pramanik and Basu (2010)
n	dimensionless	12	Eq. (1)
N	dimensionless	3.857×10^{-13}	Pramanik and Basu (2010)
M_{H_2O}	g mol^{-1}	18.01528	Pramanik and Basu (2010)
M_{EtOH}	g mol^{-1}	46.06844	Memming and Bahnemann (2015)
M_{CO_2}	g mol^{-1}	44.01	Memming and Bahnemann (2015)

5. NUMERICAL RESULTS

A code in Fortran90 was developed for the solution of equations (7), (8) and (9), as shown in the Fig.2.

The finite difference method was used for the discretization of the derivatives. The mesh employed to obtain the numerical results contains $50\times100\times100$ cells. The Fig. 3(a) refers to a cut in the middle of the fuel cell and shows the contour lines of velocity, for ethanol flow rate of 1.0 ml min^{-1} and pressure of $p = 1$ bar at the anode. The flow is laminar in all layers of the cell, having decrease of velocity at the end of the input channel until to the beginning of the output channel. This behavior is expected because the diffusion layer has larger area compared to that of the channels. The fluid follows a parabolic profile in practically all channel. Fig. 3(b) shows a zoom of the contour lines at the beginning of the diffusion layer and at the end of the input channel, with the velocity vectors for better visualization of the flow direction.

Figure 4 shows the mole fraction of ethanol, water and carbon dioxide for two different current density values. The ethanol and water react to form the product carbon dioxide. These results show that the diffusion layer contributes to resistance of the total mass transfer. The mole fraction of ethanol and water remain constant along of the input channel, and decreases in the diffusion layer and on the catalyst surface. Similarly, the mole fraction of carbon dioxide present higher formation on the electrode surface, where the electrooxidation reactions take place.

Finally, the Fig. 5 shows the current density versus cell voltage for feed of 1 M ethanol concentration for two different cell temperatures at the anode and cathode. In the first test case is considered the temperature of 315K at the anode and cathode and in the second case the temperature is 363K at the anode and 333K at the cathode. Fig. 5 also shows the cell voltage increase with the increase of temperature for given values of current density. Obtained results are in good agreement with experimental data given by Pramanik and Basu (2010).

6. CONCLUSIONS

In this work, it was developed a three-dimensional model for direct ethanol fuel cells. The reactive flow was solved based on the Navier-Stokes equations for the flow, and for the mass fraction of each species, considering losses overpotentials for anode and cathode sides. The discretization of reactive flow equations was done based on the central finite difference method, and these equations were integrated in time using the simplified three-stage explicit Runge-Kutta

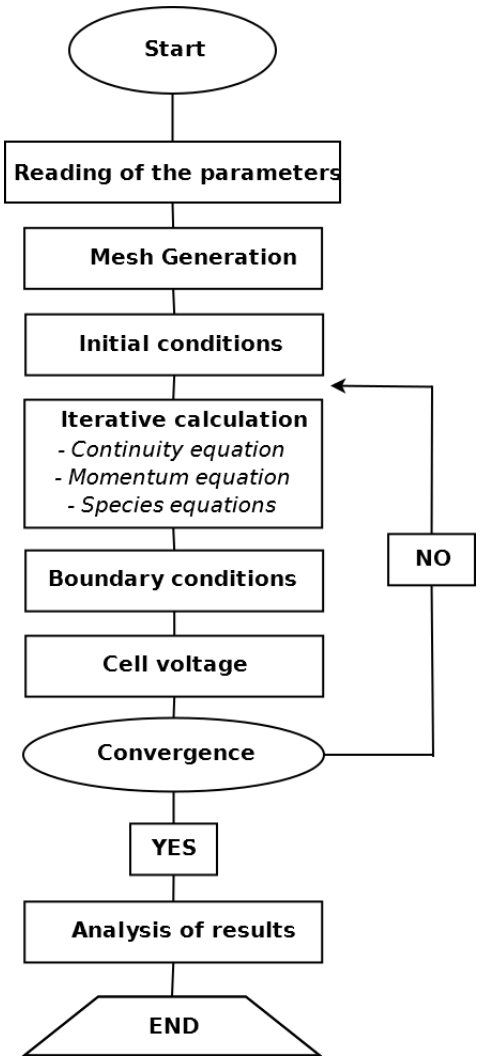

Fig. 2: Structure of the code in Fortran90.

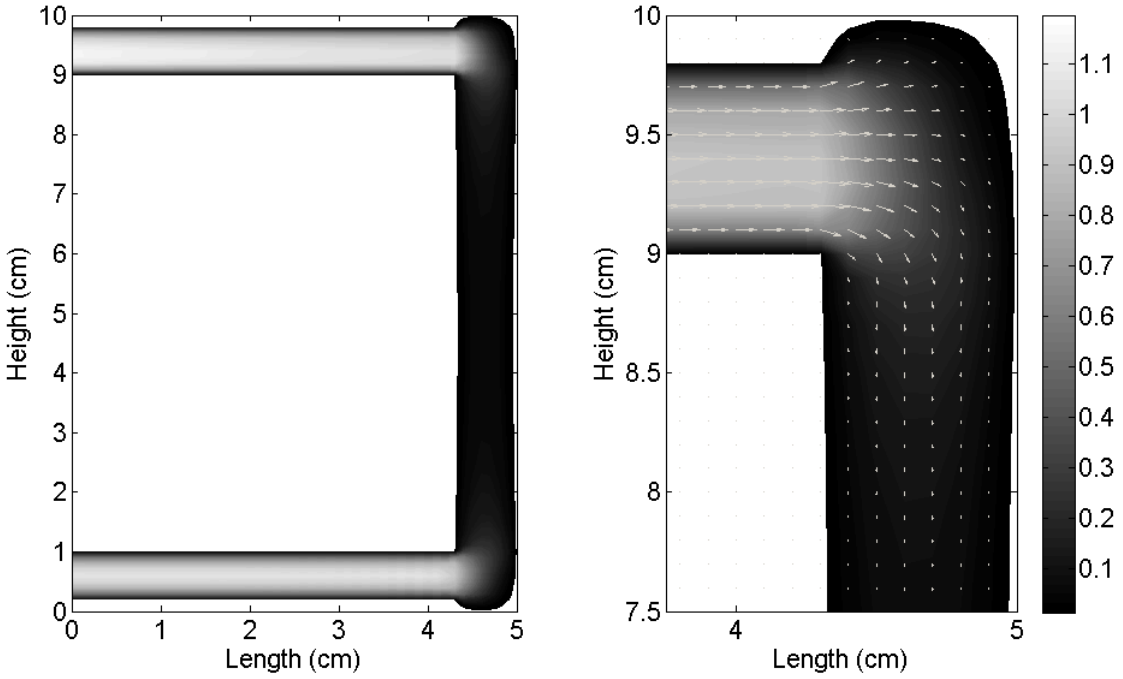

(a) Contour lines. (b) Zoom.

Fig. 3: Velocity contour lines inside the cell (anode side).

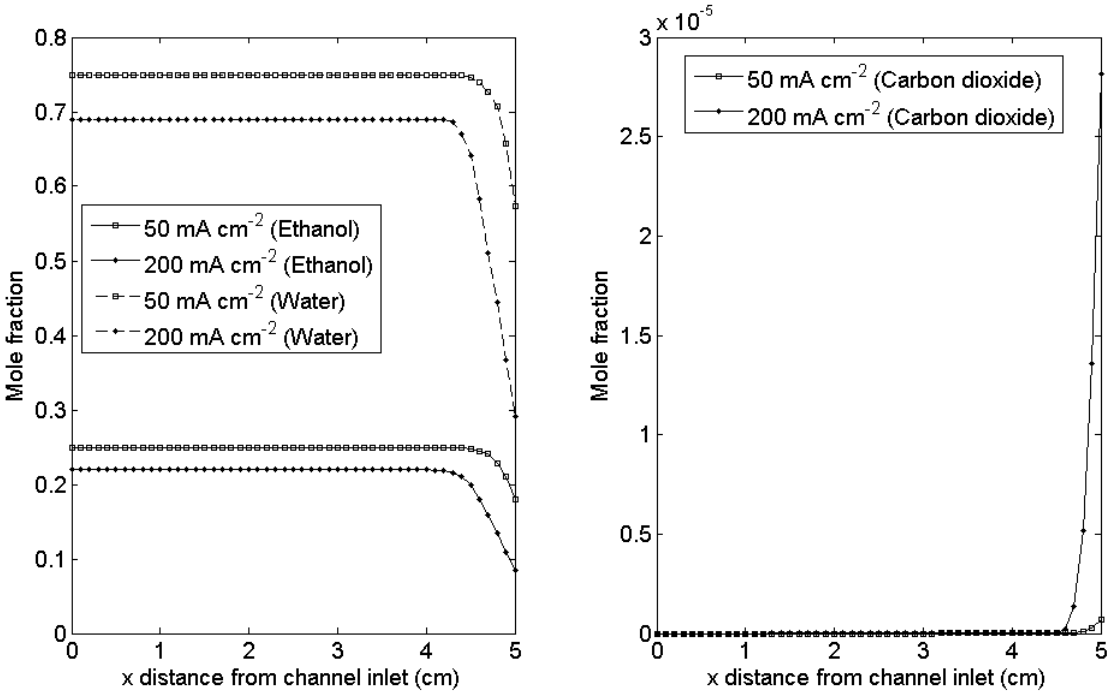

(a) Ethanol and water mole fractions.

(b) Carbon dioxide mole fraction.

Fig. 4: Mole fraction of ethanol, water and carbon dioxide for cell temperature of 373 K, ethanol feed concentration of 1 M, and ethanol flow rate of 1.0 ml min^{-1}.

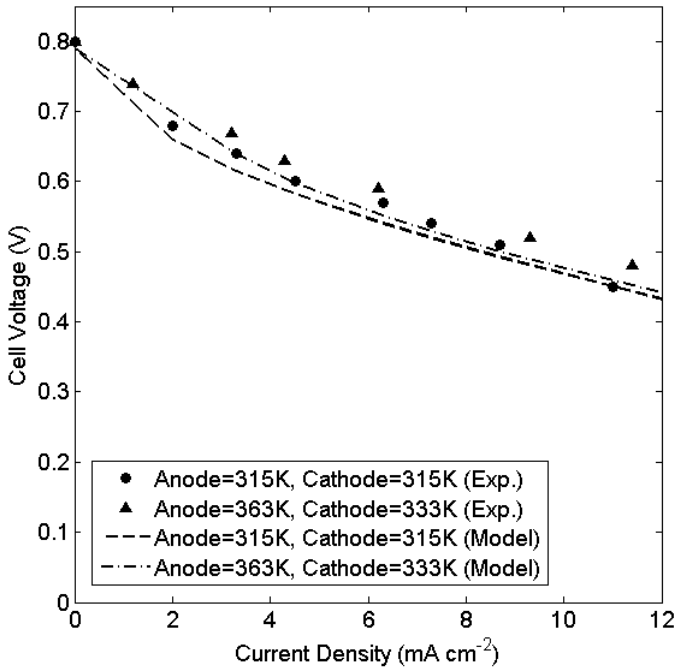

Fig. 5: Current density versus cell voltage for two cell temperatures and 1 M ethanol concentration.

scheme. Obtained results are in agreement with experimental data found in the literature for two different cell temperatures. As most of the work found in the literature is focused on one-dimensional fuel cell models, this work contributes with the development of a three-dimensional mathematical model for direct ethanol fuel cells considering all losses. Moreover, it is shown the mole fraction variations for ethanol, water and carbon dioxide in front of the membrane, what is not frequently found in the literature.

7. ACKNOWLEDGEMENTS

This research is being developed at the Universidade Federal do Rio Grande do Sul - UFRGS. Gomes and Prof. De Bortoli gratefully acknowledges the financial support from Conselho Nacional de Desenvolvimento Científico e Tecnológico - CNPq - Brazil, under the process 303816/2015-5.

8. REFERENCES

Abdullah, S., Kamarudin, S., Hasran, U., Masdar, M. and Daud, W., 2014. "Modeling and simulation of a direct ethanol fuel cell: An overview". *Journal of Power Sources*, Vol. 262, pp. 401 – 406.

Abdullah, S., Kamarudin, S., Hasran, U., Masdar, M. and Daud, W., 2015. "Development of a conceptual design model of a direct ethanol fuel cell (DEFC)". *International Journal of Hydrogen Energy*, Vol. 40, No. 35, pp. 11943 – 11948.

Al-Baghdadi, M.A., 2005. "Modelling of proton exchange membrane fuel cell performance based on semi-empirical equations". *Renewable Energy*, Vol. 30, No. 10, pp. 1587–1599.

Andreadis, G., Song, S. and Tsiakaras, P., 2006. "Direct ethanol fuel cell anode simulation model". *Journal of Power Sources*, Vol. 157, No. 2, pp. 657 – 665.

Andreadis, G., Podias, A. and Tsiakaras, P., 2008. "The effect of the parasitic current on the direct ethanol PEM fuel cell operation". *Journal of Power Sources*, Vol. 181, No. 2, pp. 214 – 227.

Bard, A.J., Faulkner, L.R. *et al.*, 2001. "Fundamentals and applications". *Electrochemical Methods, 2nd ed.; Wiley: New York*.

Colmati, F., Antolini, E. and Gonzalez, E.R., 2006. "Effect of temperature on the mechanism of ethanol oxidation on carbon supported Pt, PtRu and Pt3Sn electrocatalysts". *Journal of Power Sources*, Vol. 157, No. 1, pp. 98 – 103.

Farhat, Z.N., 2004. "Modeling of catalyst layer microstructural refinement and catalyst utilization in a PEM fuel cell". *Journal of Power Sources*, Vol. 138, No. 1, pp. 68–78.

Ge, J. and Liu, H., 2006. "A three-dimensional mathematical model for liquid-fed direct methanol fuel cells". *Journal of Power Sources*, Vol. 160, No. 1, pp. 413 – 421.

Goel, J. and Basu, S., 2015. "Mathematical modeling and experimental validation of direct ethanol fuel cell". *International Journal of Hydrogen Energy (2015)*.

Heysiattalab, S. and Shakeri, M., 2011. "2D analytical model for direct ethanol fuel cell performance prediction". *Smart Grid and Renewable Energy*, Vol. 2, No. 04, p. 427.

Kareemulla, D. and Jayanti, S., 2009. "Comprehensive one-dimensional, semi-analytical, mathematical model for liquid-feed polymer electrolyte membrane direct methanol fuel cells". *Journal of Power Sources*, Vol. 188, No. 2, pp. 367 – 378.

Lamy, C., Coutanceau, C. and Leger, J.M., 2009. *The Direct Ethanol Fuel Cell: a Challenge to Convert Bioethanol Cleanly into Electric Energy*, Wiley-VCH Verlag GmbH & Co. KGaA, pp. 1–46. ISBN 9783527625413.

Le, A.D., Zhou, B., Shiu, H.R., Lee, C.I. and Chang, W.C., 2010. "Numerical simulation and experimental validation of liquid water behaviors in a proton exchange membrane fuel cell cathode with serpentine channels". *Journal of Power Sources*, Vol. 195, No. 21, pp. 7302 – 7315. ISSN 0378-7753.

Liu, W. and Wang, C.Y., 2007. "Three-dimensional simulations of liquid feed direct methanol fuel cells". *Journal of the Electrochemical Society*, Vol. 154, No. 3, pp. B352–B361.

Memming, R. and Bahnemann, D., 2015. *Semiconductor electrochemistry*. John Wiley & Sons.

Pramanik, H. and Basu, S., 2010. "Modeling and experimental validation of overpotentials of a direct ethanol fuel cell". *Chemical Engineering and Processing: Process Intensification*, Vol. 49, No. 7, pp. 635 – 642.

Sarris, I., Tsiakaras, P., Song, S. and Vlachos, N., 2006. "A three-dimensional CFD model of direct ethanol fuel cells: Anode flow bed analysis". *Solid State Ionics*, Vol. 177, No. 19–25, pp. 2133 – 2138. Solid State Ionics 15: Proceedings of the 15th International Conference on Solid State Ionics, Part I.

Suresh, N. and Jayanti, S., 2011. "Cross-over and performance modeling of liquid-feed polymer electrolyte membrane direct ethanol fuel cells". *International Journal of Hydrogen Energy*, Vol. 36, No. 22, pp. 14648 – 14658.

Yuan, X.Z.R., Song, C., Wang, H. and Zhang, J., 2009. *Electrochemical impedance spectroscopy in PEM fuel cells: fundamentals and applications*. Springer Science & Business Media.

9. RESPONSIBILITY NOTICE

The authors are the only responsible for the printed material included in this paper.